JACS
JOURNAL OF THE AMERICAN CHEMICAL SOCIETY
Article
pubs.acs.org/JACS

Evidence of Nonelectrochemical Shift Reaction on a CO-Tolerant High-Entropy State Pt−Ru Anode Catalyst for Reliable and Efficient Residential Fuel Cell Systems

Tatsuya Takeguchi,*[,†] Toshiro Yamanaka,[†] Kiyotaka Asakura,[†] Ernee Noryana Muhamad,[†] Kohei Uosaki,[‡] and Wataru Ueda[†]

[†]Catalysis Research Center, Hokkaido University, Sapporo 001-0021, Japan

[‡]International Center for Materials Nanoarchitectonics (MANA) and Global Research Center for Environment and Energy based on Nanomaterials Science (GREEN), National Institute for Materials Science, 1-1 Namiki, Tsukuba 305-0044, Japan

Supporting Information

ABSTRACT: A randomly mixed monodispersed nanosized Pt−Ru catalyst, an ultimate catalyst for CO oxidation reaction, was prepared by the rapid quenching method. The mechanism of CO oxidation reaction on the Pt−Ru anode catalyst was elucidated by investigating the relation between the rate of CO oxidation reaction and the current density. The rate of CO oxidation reaction increased with an increase in unoccupied sites kinetically formed by hydrogen oxidation reaction, and the rate was independent of anode potential. Results of extended X-ray absorption fine structure spectroscopy showed the combination of $N_{Pt-Ru}/(N_{Pt-Ru} + N_{Pt-Pt}) \doteqdot M_{Ru}/(M_{Pt} + M_{Ru})$ and $N_{Ru-Pt}/(N_{Ru-Pt} + N_{Ru-Ru}) \doteqdot M_{Pt}/(M_{Ru} + M_{Pt})$, where $N_{Pt-Ru}(N_{Ru-Pt})$, $N_{Pt-Pt}(N_{Ru-Ru})$, M_{Pt}, and M_{Ru} are the coordination numbers from Pt(Ru) to Ru(Pt) and Pt (Ru) to Pt (Ru) and the molar ratios of Pt and Ru, respectively. This indicates that Pt and Ru were mixed with a completely random distribution. A high-entropy state of dispersion of Pt and Ru could be maintained by rapid quenching from a high temperature. It is concluded that a nonelectrochemical shift reaction on a randomly mixed Pt−Ru catalyst is important to enhance the efficiency of residential fuel cell systems under operation conditions.

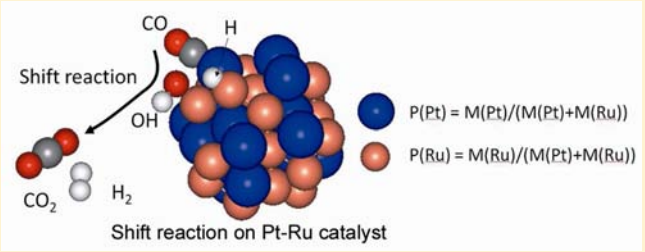

INTRODUCTION

It is expected that residential fuel cell [polymer electrolyte fuel cell (PEFC)] systems will expand markedly, since fuel cell systems are expected to contribute to reduction of CO_2 emission and their efficiency of power generation is theoretically higher than that of the Carnot cycle. However, there are many processes in fuel cell systems, and the actual efficiency is much lower than the theoretical efficiency of 83% [Δ_cG/Δ_cH = 237/286 (kJ/kJ) = 1.23/1.48 (V/V), where Δ_cG and Δ_cH are Gibbs energy and enthalpy for hydrogen combustion, respectively]. To achieve the target of distributed power sources in 2020 for the United States Department of Energy (DOE),[1] efficiency should be at least 45%; this means that cell voltage should be over 0.7 V (1.48 V × 0.45) at a current density of over 0.2 A/cm^2, at which anode potential is usually less than 0.2 V. Generally, reformate H_2 gas produced from city gas composed of CH_4 is used as fuel. Since CO is contained in reformate H_2, the anode catalyst is deactivated by the adsorption of CO. CO must be oxidized on the anode Pt−Ru catalyst[2−4] at an anode potential of less than 0.2 V. The commercial PtRu/C catalyst TEC61E54 from Tanaka Precious Metals (PtRu/C(CM), which has a relatively high probability of Pt−Ru bonding,[5] has much higher performance than that of other commercial catalysts (e.g., PtRu/C(LP) Pt:Ru = 1:1), and it is exclusively used in practice. Randomly mixed Pt−Ru catalysts are ideal catalysts for CO oxidation, but it is difficult to make such catalysts because Pt−Ru systems prefer homobonding,[5,6] owing to different stable structures.[7−9] Enthalpy tends to be the driving force at a low temperature, while entropy tends to be the driving force at a high temperature ($G = H - TS$). A high-entropy state of dispersion of Pt and Ru (random dispersion) at high temperature is maintained by rapid quenching from a high temperature. We recently prepared a randomly mixed PtRu/C [PtRu/C(RM)].[10]

A catalyst composed of highly dispersed small PtRu particles with CO tolerance higher than that of PtRu/C(CM) was obtained. Owing to the high CO tolerance of a randomly mixed monodispersed nanosized Pt−Ru catalyst, it should be possible to eliminate the CO preferential oxidation unit for a residential PEFC system and thus reduce the cost of the system. The mechanism of the CO oxidation reaction has for a long time been considered to be a bifunctional electrochemical mechanism.[2,3] This is one of the most prominent mechanisms in electrochemistry.[11] However, CO is not electrochemically oxidized at an anode potential of less than 0.35 V.[11] The anode

Received: May 21, 2012
Published: August 9, 2012

dx.doi.org/10.1021/ja304939q | J. Am. Chem. Soc. 2012, 134, 14508−14512

potential in a practical fuel cell under operation conditions is below 0.2 V, much lower than 0.35 V.[12] Therefore, we assessed the validity of this mechanism using a highly active catalyst. In this study, we tried to elucidate the mechanism of the CO oxidation reaction under operation conditions of the cell. The dependence of CO oxidation reaction rate on current and potential was analyzed to distinguish electrochemical and nonelectrochemical CO oxidation reactions (catalytic shift reaction). In addition, structures of anode catalysts were analyzed by extended X-ray absorption fine structure spectroscopy (EXAFS), and the results are discussed in relation to performance of the anode catalyst. It is concluded that the nonelectrochemical shift reaction is the main mechanism for CO oxidation of an anode catalyst under operation conditions.

EXPERIMENTAL SECTION

PtRu/C(RM) catalysts of Pt:Ru = 2:3 were prepared. First, 40 wt % Pt/C, $RuCl_3{\cdot}nH_2O$, methanol, and distilled water were mixed and stirred in a glass bottle at boiling point. During this process, Ru was reduced by methanol and adhered to Pt/C. The molar ratios of Pt:Ru in the catalysts and $RuCl_3{\cdot}nH_2O$ were 2:3. After 12 h of stirring, the catalysts obtained were filtered and washed with hot distilled water. Then the catalysts were dried in air at 80 °C overnight. Next, the catalysts were reduced in H_2/Ar (5% H_2) during rapid heating to 900 °C within 10 min. The oven was turned off immediately when the temperature had reached 900 °C to rapidly cool the catalyst. The temperature decreased from 900 to 500 °C in 18 min and decreased from 500 °C to room temperature in about 50 min.

For preparation of a membrane electrode assembly (MEA), carbon paper was used as the backing layers of the anode and cathode. Anode catalysts [PtRu/C(CM) (Pt:Ru = 2:3 (molar ratio)), PtRu/C(RM) (Pt:Ru = 2:3 (molar ratio), PtRu/C(LP) Pt:Ru = 1:1 (molar ratio), and $Pt/MoO_x/C$][13] and nafion solution were ultrasonically suspended in water. The carbon paper was painted with the resultant catalyst ink. The loading of PtRu in the anode catalyst layer was 0.5 mg cm^{-2}. In all cases, an identical cathode catalyst layer was prepared by the same procedure. A commercial Pt/C cathode catalyst (40 wt % Pt) was used instead of PtRu/C catalysts, and the loadings of Pt in the resultant cathode layer were 0.5 mg cm^{-2}. Finally, the anode and cathode (22 × 22 mm) were placed onto the two sides of a nafion NRE-212 membrane (Aldrich) and hot-pressed at 135 °C and 4 MPa for 10 min to form the MEA. The MEA was assembled into a single cell with flow field plates made of graphite and copper end plates attached to a heater (FC05-01SP, ElectroChem, Inc.). The single cell was connected to fuel cell test equipment (Chino Corp.). Pure H_2 (or H_2/CO mixture) and O_2 were supplied at flow rates of 80 mL min^{-1} to the anode and cathode, respectively, at ambient pressure. During the measurement, a single cell was operated at 75 °C, and the anode and cathode humidifiers were set at 75 and 70 °C, respectively. CO_2 concentration of the exhaust gas from the anode side of the cell was analyzed by an online micro gas chromatograph, Varian CP 4900, with thermal conductivity detectors. The local structures were determined by EXAFS analyses. Pt LIII- and Ru K-edges X-ray absorption spectra were measured at beamlines BL-7C and NW-10A of Photon Factory of IMSS-KEK (Proposal number: 2009U002). Experimental details of the EXAFS analyses are described elsewhere.[14]

RESULTS AND DISCUSSION

Since precise description of reactions on surfaces of real catalysts is difficult, we apply simplified description as follows: During the operation of fuel cells, humidified H_2 with dilute CO is fed onto the anode. Under the condition of an open circuit (without power generation), the following reactions proceed. Since the pressure of H_2 is higher than the pressure of H_2O and CO in the anode gas, H_2 is first adsorbed on an empty site of the Pt−Ru alloy.[2,3]

$$1/2H_2 + S(Pt{-}Ru) \rightleftarrows H{-}S(Pt{-}Ru) \quad (1)$$

S(Pt−Ru) is a surface site on the Pt−Ru alloy, while H−S(Pt−Ru) is H adsorbed on the Pt−Ru alloy. When H_2O is dissociatively adsorbed on the Pt−Ru alloy by catalytic reaction 2 or electrocatalytic reaction 3, OH is selectively adsorbed on a surface site of Ru, owing to the thermodynamic stability.[3]

$$H_2O + 2S(Pt{-}Ru) \rightleftarrows H{-}S(Pt{-}Ru) + OH{-}S(Ru) \quad (2)$$

$$H_2O + S(Pt{-}Ru) \rightleftarrows OH{-}S(Ru) + H^+ + e^- \quad (3)$$

OH−S(Ru) is OH selectively adsorbed on a surface site of Ru. OH−S(Ru) is not fomed by electrocatalytic reaction under a potential lower than 0.35 V by electrochemical reaction 3,[3] while OH−S(Ru), as a reactive intermediate, can be fomed by reaction 2, an elementary reaction for thermodynamically advantageous shift reaction. Since the pressure of CO is much lower than the pressure of H_2 and H_2O, adsorbed hydrogen is gradually replaced by CO, owing to the thermodynamic stability of adsorbed CO on the Pt−Ru alloy.[15]

$$CO + H{-}S(Pt{-}Ru) \rightarrow CO{-}S(Pt{-}Ru) + 1/2H_2 \quad (4)$$

CO−S(Pt−Ru) is CO adsorbed on a surface site of the Pt−Ru alloy. Under an open circuit condition without electrochemical reaction, the flowing shift reaction 5 takes place by way of reaction 6,[16] yielding an empty site [S(Pt−Ru)].

$$CO + H_2O \rightarrow H_2 + CO_2 \quad (5)$$

$$CO{-}S(Pt{-}Ru) + OH{-}S(Ru) \rightarrow CO_2 + 1/2H_2 + 2S(Pt{-}Ru) \quad (6)$$

The number of empty sites [S(Pt−Ru)] decreases with an increase in time, because the forward side reaction of reaction 1 is favorable. Thus, reaction 2 stops and OH−S(Ru) disappears with increase in time [OH coverage (θ_{OH}(Ru) becomes zero]. Therefore, the rate of the shift reaction is almost zero in a steady state.

During power generation (closed circuit), electrons are emitted by hydrogen oxidation reaction 7, yielding empty sites [S(Pt−Ru)].

$$H{-}S(Pt{-}Ru) \rightarrow S(Pt{-}Ru) + H^+ + e^- \quad (7)$$

Thus, the number of empty sites increases with an increase in current (relation 8).

$$\theta_{emp}(Pt{-}Ru) \propto I \quad (8)$$

θ_{emp}(Pt−Ru) and I are the probability of a kinetically formed empty site of the Pt−Ru alloy and current density generated by reaction 7, respectively. As mentioned above, θ_{emp}(Pt−Ru) and θ_{OH}(Ru) in a steady state are 0 with I of 0. Therefore, θ_{emp}(Pt−Ru) is expected to be proportional to I (relation 8). On the other hand, OH on Ru is formed by reaction 2, which needs two empty sites [S(Pt−Ru)]. Thus, OH coverage [θ_{OH}(Ru)] is proportional to I^2.

$$\theta_{OH}(Ru) \propto \theta_{emp}(Pt{-}Ru)^2 \propto I^2 \quad (9)$$

If the bifunctional mechanism is assumed, adsorbed CO is expected to be electrochemically oxidized according to the following reaction 10:[2,3]

dx.doi.org/10.1021/ja304939q | J. Am. Chem. Soc. 2012, 134, 14508−14512

$$\mathrm{OH{-}S(Ru)} + \mathrm{CO{-}S(Pt{-}Ru)} \rightarrow \mathrm{CO_2} + \mathrm{H^+} + \mathrm{e^-} + 2\mathrm{S(Pt{-}Ru)} \quad (10)$$

CO is continuously eliminated by reaction 10, and P_{CO} is low. Thus, CO coverage of PtRu [θ_{CO}(Pt−Ru)] is small. CO can be adsorbed on any sites.[2,3] In this case, θ_{CO}(Pt−Ru) at equilibrium is proportional to P_{CO} (pressure of CO) under a constant current condition.

$$\theta_{CO}(\mathrm{Pt{-}Ru}) \propto P_{CO} \quad (11)$$

The rate of CO oxidation reaction (r_{CO_2}) is proportional to θ_{CO}(Pt−Ru)θ_{OH}(Ru)exp(aE) (relation 12a and equation 12b), where a and E are a constant and anode potential, respectively.

$$r_{CO_2} \propto \theta_{CO}(\mathrm{Pt{-}Ru})\theta_{OH}(\mathrm{Ru})\exp(aE) \propto P_{CO}I^2\exp(aE) \quad (12a)$$

$$\ln(r_{CO_2}/P_{CO}I^2) = a\mathrm{E} + \mathrm{const} \quad (a = F/RT,\ F\text{: Faraday constant}) \quad (12b)$$

Logarithms of conversion rate ($\propto r_{CO_2}/P_{CO}$) divided by I^2 were plotted against anode potential (E) to investigate the effect of anode potential on CO electrooxidation in an MEA under operation conditions. First, the relation between overpotential on the Pt/C cathode and current density was roughly estimated in a pure H_2 system in the anode and pure O_2 in the cathode. The anode potential of PtRu/C was calculated by the corresponding cell voltage and cathode overpotential of Pt/C at the corresponding current density. The $\ln(r_{CO_2}/P_{CO}I^2)$ values seem to be independent of anode potential of E lower than 0.38 V as shown in Figure 1, which is different from equation 12b (dashed and dotted lines). Electrochemical oxidation of CO in the MEA under operation conditions is not observed.

Maillaerd et al. reviewed CO electrooxidation on PtRu and reported that the lowest onset potential was 0.35 V.[11] Figure 2 shows CO stripping at 60 °C for PtRu/(CM) and PtRu/C(RM). Performances of PtRu/(CM) and PtRu/C(RM) for electrochemical oxidation are almost the same as those of the highest-performance PtRu catalysts reviewed. The potential range of electrochemical CO oxidation (>0.35 V in Figure 2) is higher than the range of anode potential under practical operation conditions (<0.38 V in Figure 1), indicating different oxidation mechanisms. The effect of CO concentration on cell voltage at 0.2 A/cm^2 is shown in Figure 3, and various catalysts show different degrees of CO tolerance. PtRu/C(RM) shows the highest cell voltage over 0.7 V with an anode potential as low as 0.14 V at 0.2 A/cm^2 in the presence of 500 ppm CO under practical operation conditions. From a comparison of Figures 2 and 3, CO tolerance is independent of the performance for electrochemical CO oxidation reaction.

Therefore, contribution of the shift reaction to CO tolerance was evaluated. Pt generally requires higher operating temperatures of about 200 °C for the shift reaction due to lower activity for water dissociation on Pt and strong CO binding without a current.[17] However, in the present case of PtRu/C under practical operation conditions, an empty site is formed by hydrogen oxidation reaction (reaction 7). Since OH can be

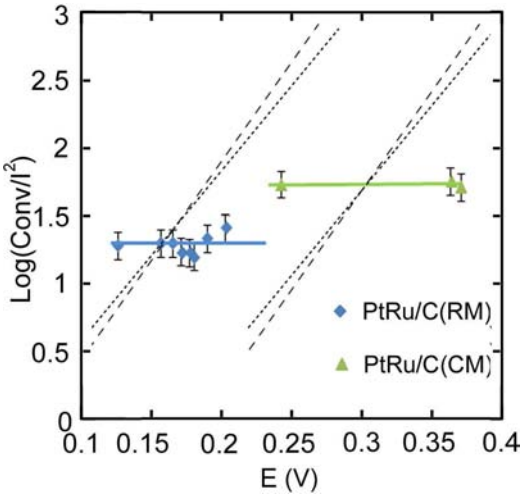

Figure 1. Dependence of CO_2 formation rate on anode potential. Logarithms of conversion rate (r_{CO_2}/P_{CO}) divided by I^2 are plotted against anode potential. PtRu/C(RM) at a cell voltage of 0.7 V (diamonds, ◆) and PtRu/C(CM) at a cell volatage over 0.46 V (triangles, ▲). The slopes expected from equation 12b) with $a = F/RT$ and a obtained by curve fitting of CO stripping (Figure 2) are shown by dashed and dotted lines, respectively.

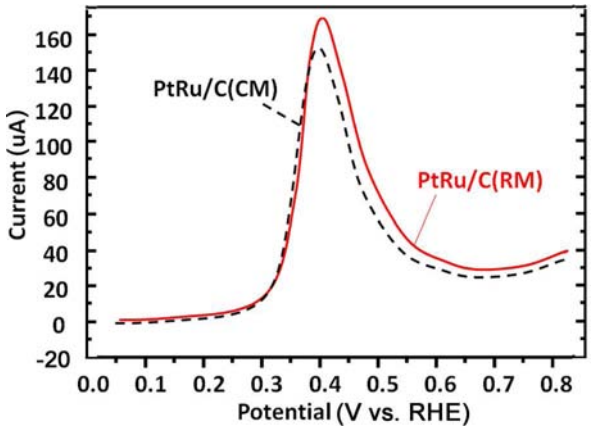

Figure 2. CO stripping at 60 °C. CO was (1) fed for 20 min at 0.05 V in 0.1 M $HClO_4$; (2) purged for 30 min; and (3) sweeped at 60 °C between 0.05 and 0.8 V at 10 mV/s.

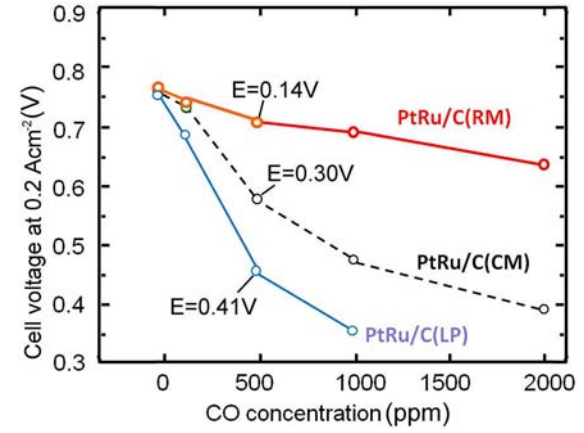

Figure 3. Effect of CO concentration on cell voltage at 0.2 A/cm^2. Cell temp.: 70 °C; electrolyte: nafion NRE 212; cathode: Pt/C (0.5 mg/cm^2); O_2 humidified at 70 °C; flow rate: 80 mL/min; anode: Pt_2Ru_3/C (0.5 mg PtRu/cm^2); H_2 containing 0−2000 ppm CO humidified at 70 °C; and flow rate: 80 mL/min.

dx.doi.org/10.1021/ja304939q | J. Am. Chem. Soc. 2012, 134, 14508−14512

adsorbed on Ru,[18,19] shift reaction is expected via dissociative adsorption of water.[20−26] In the case of nonelectrochemical shift reaction (reaction 6), relation 12a and equation 12b are replaced by 13a and 13b.

$$r_{CO2} \propto P_{CO} I^2 \tag{13a}$$

$$(r_{CO_2}/P_{CO})^{1/2} \propto I \tag{13b}$$

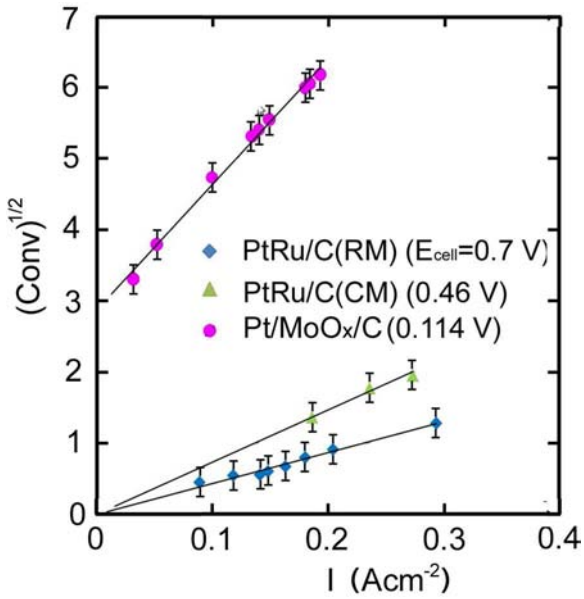

Figure 4. Dependence of conversion rate on *I*. PtRu/C(RM) at a cell voltage of 0.7 V (diamonds, ◆), PtRu/C(CM) over 0.46 V (triangles, ▲) and Pt/MoO_x/C over 0.114 V (circles, ●).

In Figure 4, the root of the conversion rate (r_{CO_2}/P_{CO}) is plotted against *I*. The values linearly increase with increase in *I*, suggesting a nonelectrochemical shift reaction. The rate of shift reaction is enhanced by an increase in the number of empty sites kinetically formed by H_2 oxidation reaction (reaction 7). When Pt and Ru are mixed well, OH−S(Ru) reacts with CO on Pt rather than with that on Ru. Shift reaction on Pt−Ru is dominant, and it effectively contributes to CO tolerance. On the other hand, when Pt and Ru are not mixed well, OH−S(Ru) reacts with CO on Ru rather than with that on Pt. Shift reaction on Ru is dominant, and its contribution to CO tolerance is small. Since hydrogen oxidation reaction mainly occurs on Pt, it is necessary to eliminate CO on Pt to obtain a high CO tolerance.

In this study, Pt/MoO_x/C was used as a low-alloy model catalyst since shift reaction on MoO_x is dominant, with little contribution to CO tolerance. It is known that shift reaction occurs on various metal oxides in H_2O + CO (or H_2O + H_2 + CO). The most probable mechanism is thought to be reaction between CO and OH produced by dissociative adsorption of water.[20−26] This mechanism can be described in the case of Pt/MoO_x/C) as follows, similar to reactions 1−4 and 6.

$$1/2H_2 + S(Pt{-}Mo) \rightleftarrows H{-}S(Pt{-}Mo) \tag{14}$$

$$H_2O + 2S(Pt{-}Mo) \rightleftarrows OH{-}S(Mo) + H{-}S(Pt{-}Mo) \tag{15}$$

$$CO + S(Pt{-}Mo) \rightleftarrows CO{-}S(Pt{-}Mo) \tag{16}$$

$$OH{-}S(Mo) + CO{-}S(Pt{-}Mo) \rightarrow CO_2 + 2S(Pt{-}Mo) + 1/2H_2 \tag{17}$$

S(Pt−Mo) is a surface site of Pt/MoO_x, while OH−S(Mo) and CO−S(Pt−Mo) are OH selectively adsorbed on a surface site of MoO_x and CO adsorbed on a surface site of Pt/MoO_x, respectively. Even without a current, a large amount of OH is adsorbed on MoO_x. Therefore, shift reaction 17 proceeds, yielding an empty site [S(Pt−Mo)] without a current. With an increase in density of the current generated by hydrogen oxidation reaction (reaction 18), the number of empty sites increases.

$$H{-}S(Pt{-}Mo) \rightleftarrows S(Pt{-}Mo) + H^+ + e^- \tag{18}$$

$$\theta_{emp}(Pt{-}Mo) = b(1 + k_I I) \quad (b \text{ and } k_I \text{ are constants}) \tag{19}$$

θ_{emp}(Pt−Mo) is probability of a kinetically formed empty site of Pt/MoO_x. As mentioned above, θ_{emp}(Pt−Mo) has an intercept *b* without a current. The rate of CO oxidation reaction (r_{CO_2}) is described as follows:

$$r_{CO_2} \propto P_{CO}\theta_{OH}(Mo) \propto P_{CO}\theta_{emp}(Pt{-}Mo)^2 \propto P_{CO} b^2 (1 + k_I I)^2 \tag{20a}$$

$$(r_{CO_2}/P_{CO})^{1/2} \propto \theta_{emp}(Pt{-}Mo) \propto b(1 + k_I I) \tag{20b}$$

In Figure 4, the root of conversion rate for Pt/MoO_x/C is expressed well by relation 20b, suggesting a nonelectrochemical shift reaction. Pt/MoO_x/C showed much lower CO tolerance than that of PtRu/C(RM) (cell voltage at 500 ppm CO and 0.2 Acm^{-2} was zero for Pt/MoO_x/C, while PtRu/C(RM) and PtRu/C(CM) showed 0.72 and 0.58 V, respectively). Shift reaction does not effectively contribute to CO tolerance. CO on MoO_x is oxidized by shift reaction more effectively than is CO on Pt.

The PtRu catalyst with a low alloy degree showed the same tendency. CO on Ru was oxidized by shift reaction more effectively than was CO on Pt, and CO tolerance was low (cell voltage at 500 ppm and 0.2 Acm^{-2} was zero). Detailed kinetic analysis indicated that CO_2 is formed by a shift reaction under practical conditions. Pt−Ru bonding is important to remove CO on Pt in order to achieve high CO tolerance. Electrochemical CO oxidation reaction did not progress under practical conditions. This indicated that CO is oxidized by the shift reaction between CO on the Pt−Ru alloy and OH on Ru. The most important factor of the Pt−Ru system is the probability of Pt−Ru bonding, since shift reaction on a single Ru site did not directly contribute to CO tolerance.

Pt has an fcc structure, while Ru has an hcp structure;[7−9] therefore, bondings between like atoms (Pt−Pt and Ru−Ru bondings) were more preferably formed than were bondings between unlike atoms (Pt−Ru bonding).[5,6] Actually, ratios of $N_{Pt-Ru}/(N_{Pt-Ru} + N_{Pt-Pt})$ (0.44) and $N_{Ru-Pt}/(N_{Ru-Pt} + N_{Ru-Ru})$ (0.32) for PtRu/C(CM) obtained from results of EXAFS were less than those expected from a randomly mixed case, where

dx.doi.org/10.1021/ja304939q | J. Am. Chem. Soc. 2012, 134, 14508−14512

N_{Pt-Ru} (N_{Ru-Pt}) is the coordination number from Pt(Ru) to Ru(Pt), and N_{Pt-Pt} (N_{Ru-Ru}) is the coordination number from Pt (Ru) to Pt (Ru). On the other hand, PtRu/C(RM) shows the combination of $N_{Pt-Ru}/(N_{Pt-Ru} + N_{Pt-Pt})$ of 0.59 ≒ $M_{Ru}/(M_{Pt} + M_{Ru})$ of 0.60 and $N_{Ru-Pt}/(N_{Ru-Pt} + N_{Ru-Ru})$ of 0.37 ≒ $M_{Pt}/(M_{Ru} + M_{Pt})$ of 0.40, where M_{Pt} and M_{Ru} are molar ratios of Pt and Ru, respectively. This indicates that Pt and Ru atoms are mixed with an almost completely random distribution in the high-temperature melt, and the random distribution of Pt and Ru atoms formed is retained by rapid quenching. This is the first report of a completely randomly distributed PtRu alloy catalyst with high-entropy state. The CO tolerance of PtRu/C(RM) is much higher than that of PtRu/C(CM), since PtRu/C(RM) has more Pt−Ru bondings.

In summary, the rate of CO oxidation on a PtRu/C anode catalyst of a PEFC was proportional to the square of current density and independent of anode potential. CO tolerance of anode catalysts under practical conditions of a PEFC was independent of activities for electrochemical CO oxidation. It is concluded that a nonelectrochemical shift reaction on a completely randomly mixed Pt−Ru catalyst contributes to CO removal, resulting in enhancement of the efficiency of residential fuel cell systems. The present results have implication for understanding of the CO tolerance mechanism and development of a high-performance anode catalyst and other poison-tolerant catalysts.

■ ASSOCIATED CONTENT

Supporting Information

CO pressure dependence of CO_2 formation, electrochemical CO oxidation at high anode potential, and structure analysis by EXAFS. This material is available free of charge via the Internet at http://pubs.acs.org.

■ AUTHOR INFORMATION

Corresponding Author

takeguch@cat.hokudai.ac.jp

Notes

The authors declare no competing financial interest.

■ ACKNOWLEDGMENTS

This work was partly supported by the New Energy and Industrial Technology Development Organization (NEDO) Japan.

■ REFERENCES

(1) *2010 DOE Hydrogen and Fuel Cells Program Plan Draft*; Department of Energy: Washington, DC, 2010; pp 9−33.

(2) Watanabe, M.; Motoo, S. *J. Electroanal. Chem. Interfacial Electrochem.* **1975**, *60*, 267−273.

(3) Watanabe, M.; Motoo, S. *J. Electroanal. Chem. Interfacial Electrochem.* **1975**, *60*, 275−283.

(4) Roth, C.; Benker, N.; Buhrmester, T.; Mazurek, M.; Loster, M.; Fuess, H.; Koningsberger, D. C.; Ramaker, D. E. *J. Am. Chem. Soc.* **2005**, *127*, 14607−14615.

(5) Yamamoto, T. A.; Kageyama, S.; Seino, S.; Nitani, H.; Nakagawa, T.; Horioka, R.; Honda, Y.; Ueno, K.; Daimon. *Appl. Catal., A* **2011**, *396*, 68−75.

(6) Nitani, H.; Nakagawa, T.; Daimon, D.; Kurobe, Y.; Ono, T.; Honda, Y.; Koizumi, A.; Seino, S.; Yamamoto, T. A. *Appl. Catal., A* **2007**, *326*, 194−201.

(7) Antolini, E. *Mater. Chem. Phys.* **2003**, *78*, 563−573.

(8) Antolini, E.; Giorgi, L.; Cardellini, F.; Passalacqua, E. *J. Solid State Electrochem.* **2001**, 131−140.

(9) Okamoto, K. *J. Phase Equilib. Diffus.* **2008**, *29*, 471.

(10) Yamanaka, T.; Takeguchi, T.; Wang, G. X.; Muhamad, E. N.; Ueda, W. *J. Power Source* **2010**, *195*, 6398−6404.

(11) Maillard, M.; Lu, G.-Q.; Wieckowski, A.; Stimming, U. *J. Phys. Chem. B* **2005**, *109*, 16230−16243.

(12) Gasteiger, H. A.; Marković, N. M.; Ross, P. N., Jr. *J. Phys. Chem.* **1995**, *99*, 8290−8301.

(13) Muhamad, E. N.; Takeguchi, T.; Wang, F.; Wang, G. X.; Yamanaka, T.; Ueda, W. *J. Electrochem. Soc.* **2009**, *156*, B1361−B1368.

(14) Bian, C.-R.; Suzuki, S.; Asakura, K.; Ping, L.; Toshima, N. *J. Phys. Chem.* **2002**, *106*, 8587−8598.

(15) Feliu, J. M.; Orts, J. M.; Fernandez-Vega, A.; Aldaz, A.; Clavilier, J. *J. Electroanal. Chem.* **1990**, *296*, 191−201.

(16) Grabow, L. C.; Gokhale, A. A.; Evans, S. T.; Dumesic, J. A.; Mavrikakis, M. *J. Phys. Chem. C* **2008**, *112*, 4608−4617.

(17) Flaherty, D. W.; Yu, W. Y.; Pozun, Z. D.; Henkelman, G.; Mullins, C. B. *J. Catal.* **2011**, *282*, 278−288.

(18) Leavitt, P. K.; Davis, J. L.; Dyer, J. S.; Thiel, P. A *Surf. Sci.* **1989**, 346−362.

(19) Clay, C.; Haq, S.; Hodgson, A. *Chem. Phys. Lett.* **2004**, *388*, 89−93.

(20) Campbell, C. T.; Daube, K. A. *J. Catal.* **1987**, *104*, 109−119.

(21) Andreeva, D.; Idakiev, V.; Tabakova, T.; Andreev, A.; Giovanoli, R. *Appl. Catal., A* **1996**, *134*, 275−283.

(22) Saito, Y.; Terada, K.; Hasegwa, S.; Miyao, T.; Naito, S. *Appl. Catal., A* **2005**, *296*, 80−89.

(23) Azzam, K. G.; Babich, I. V.; Seshan, K.; Leffers, L. *J. Catal.* **2007**, *296*, 153−162.

(24) Rostam, J. M.; Braden, D.; Kandoi, S.; Nagel, P.; Mavrkakis, M; Dumesic, J. A. *J. Catal.* **2007**, *296*, 153−162.

(25) Shido, T.; Iwasawa, Y. *J. Catal.* **1993**, *141*, 71−81.

(26) Shido, T.; Iwasawa, Y. *J. Catal.* **1993**, *136*, 493−503.